A STUDY ON FRICTION COEFFICIENT AND WEAR COEFFICIENT OF COATED SYSTEMS SUBMITTED TO MICRO-SCALE ABRASION TESTS[1]

Ronaldo Câmara Cozza[2]
Abel André Candido Recco[3]
André Paulo Tschiptschin[4]
Roberto Martins de Souza[5]
Deniol Katsuki Tanaka[5]

Abstract

Several works on the friction coefficient during abrasive wear tests are available in the literature, but only a few were dedicated to the friction coefficient in micro-abrasive wear tests conducted with rotating ball. This work aims to study the influence of titanium nitride (TiN) and titanium carbide (TiC) coatings hardness on the friction coefficient and wear coefficient in ball-cratering micro-abrasive wear tests. A ball of AISI 52100 steel and two specimens of AISI D2 tool steel, one coated with TiN and another coated with TiC, were used in the experiments. The abrasive slurry was prepared with black silicon carbide (SiC) particles and distilled water. Two normal forces and six sliding distances were defined, and both normal and tangential forces were monitored constantly during all tests. The movement of the specimen in the direction parallel to the applied force was also constantly monitored with the help of a Linear Ruler. This procedure allowed the calculation of crater geometry, and thus the wear coefficient for the different sliding distances without the need to stop the test. The friction coefficient was determined by the ratio between the tangential and the normal forces, and for both TiN and TiC coatings, the values remained, approximately, in the same range (from μ = 0.4 to μ = 0.9). On the other hand, the wear coefficient decreased with the increase in coating hardness.

Key words: Micro-abrasive wear testing; Thin films; Friction coefficient; Wear coefficient.

UM ESTUDO SOBRE COEFICIENTE DE ATRITO E COEFICIENTE DE DESGASTE DE SISTEMAS REVESTIDOS SUBMETIDOS A ENSAIOS DE DESGASTE MICROABRASIVO

Resumo

Diversos trabalhos sobre coeficiente de atrito em ensaios de desgaste abrasivo estão disponíveis na literatura, mas poucos estão relacionados ao coeficiente de atrito gerado em ensaios de desgaste micro-abrasivo por esfera rotativa. Este trabalho objetiva estudar a influência das durezas de filmes finos de nitreto de titânio (TiN) e carbeto de titânio (TiC) sobre os coeficientes de atrito e desgaste, em ensaios "ball-cratering". Uma esfera de aço AISI 52100 e dois corpos de prova de aço-ferramenta AISI D2, um revestido com TiN e outro revestido com TiC, foram utilizados nos experimentos. A pasta abrasiva foi preparada com partículas de carbeto de silício (SiC) preto e água destilada. Duas forças normais e seis distâncias de deslizamento foram definidas, sendo as forças normal (N) e tangencial (T) monitoradas constantemente em todos os ensaios. Assim como N e T, com o auxílio de uma Régua Linear, o deslocamento (h) do corpo-de-prova, na direção paralela à aplicação da carga normal, foi continuamente medido, o que permitiu o cálculo da geometria de cada cratera de desgaste e, consequentemente, o cálculo do coeficiente de desgaste para as diferentes distâncias de deslizamento sem a necessidade de interrupção do ensaio. O coeficiente de atrito foi determinado pela relação entre as forças tangencial e normal, e para ambos revestimentos, os valores permaneceram, aproximadamente, na mesma faixa (entre μ = 0,4 e μ = 0,9). Por outro lado, o coeficiente de desgaste diminuiu com o aumento da dureza do revestimento.

Palavras-chave: Ensaio de desgaste microabrasivo; Filmes finos; Coeficiente de atrito; Coeficiente de desgaste.

1 *Technical contribution to 64th ABM Annual Congress, July, 13th to 17th, 2009, Belo Horizonte, MG, Brazil.*

2 *Doctorate Student – Polytechnic School of the University of São Paulo (USP) – Department of Mechanical Engineering.*

3 *Doctor in Metallurgic Engineering – Polytechnic School of the USP – Department of Metallurgic and Materials Engineering.*

4 *Professor – Polytechnic School of the USP – Department of Metallurgic and Materials Engineering.*

5 *Professor – Polytechnic School of the USP – Department of Mechanical Engineering.*

1 INTRODUCTION

At first, a list of symbols used in this manuscript is given.

Nomenclature

a	internal diameter of the wear crater (substrate) [mm]
b	external diameter of the wear crater (coating) [mm]
D	diameter of the ball [mm]
E_c	Young's modulus of the coating [GPa]
E_i	Young's modulus of the indenter [GPa]
E^*	reduced Young's modulus [GPa]
h	total depth of the wear crater (coating and substrate) [mm]
h_c	coating thickness [µm]
H	hardness [GPa]
k	wear coefficient [mm^3/N.m]
kc	wear coefficient of the coating [mm^3/N.m]
ks	wear coefficient of the substrate (substrate + coating) [mm^3/N.m]
kt	total wear coefficient (substrate + coating) [mm^3/N.m]
n	ball rotational speed [rpm]
N	normal force [N]
R	radius of the ball [mm]
S	sliding distance [m]
t	test time [s]
T	tangential force (friction force) [N]
v	tangential sliding velocity [m/s]
V	total wear volume (volume of the wear crater; coating and substrate) [mm^3]
V_c	wear volume of the coating [mm^3]
V_s	wear volume of the substrate [mm^3]
Greek letters	
α	significance level
μ	friction coefficient
μ_{higher}	higher friction coefficient
μ_{lower}	lower friction coefficient
ν_c	coefficient of Poisson of the coating
ν_i	coefficient of Poisson of the indenter

Recently, the micro-scale abrasive wear test has gained large acceptance in universities and research centers, being widely used in studies on the abrasive wear of materials. Figure 1a[1,2] presents a schematic diagram of the principle of this abrasive wear test, where a rotating ball is forced against the tested specimen, in the presence of an abrasive slurry. There are two main equipment configurations to conducted this type of test: "free-ball" and "fixed-ball". Figures 1b[3-5] and 1c[1,2,5-9] show examples of these equipments.

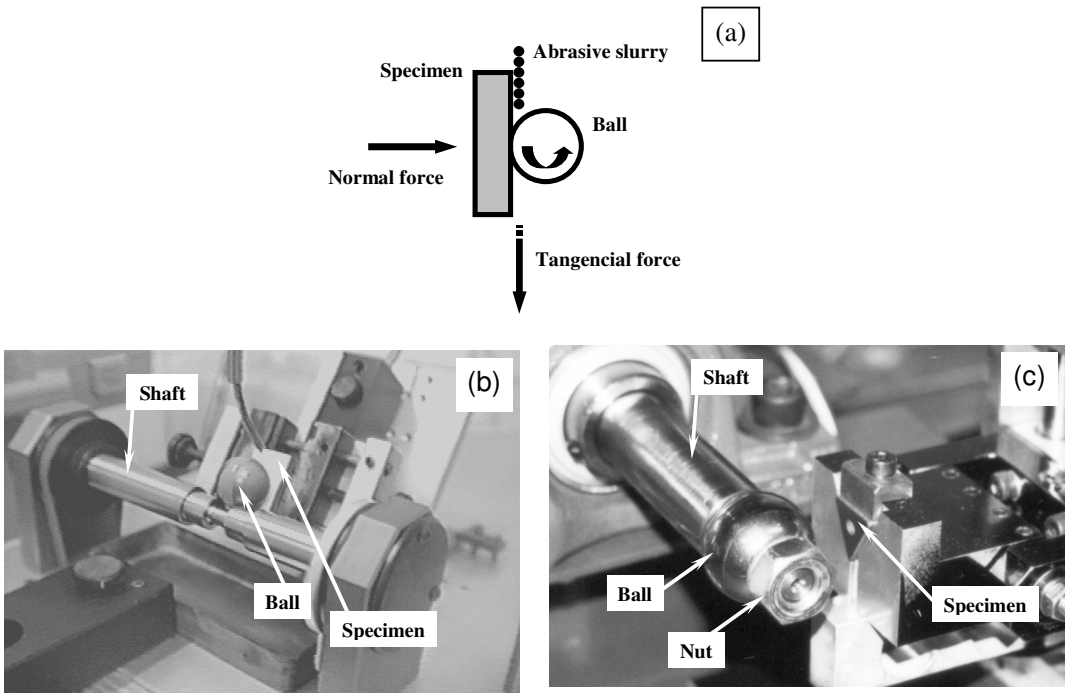

Figure 1. Micro-abrasive wear testing by rotating ball: (a) schematic diagram of its principle;[1,2] (b) "free-ball" configuration;[3-5] (c) "fixed-ball" configuration.[1,2,5-9]

The aim of the micro-abrasive wear test is to generate "wear craters" on the specimen. Figure 2 presents images of such craters when generated in coated systems, together with an indication of the total wear volume (V), the total crater depth (h), the coating thickness (h_c), the internal crater diameter (a)[9] and the external crater diameter (b).[9]

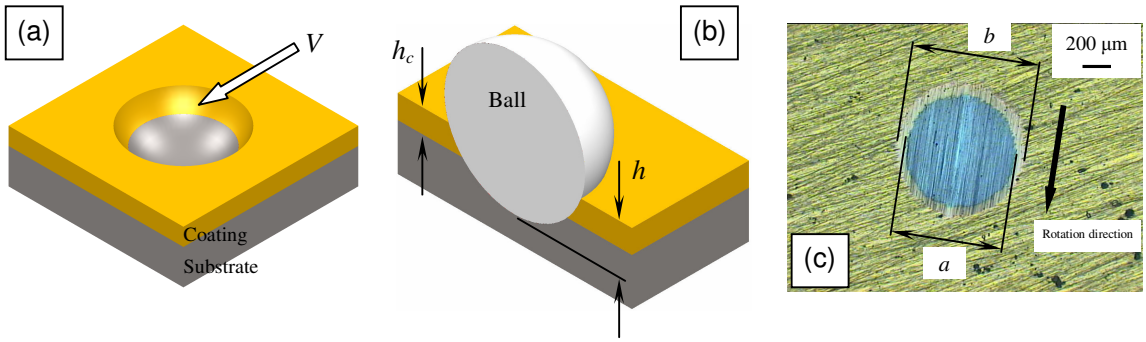

Figure 2. Images of wear craters generated in coated systems: (a) total wear volume - V (schematic illustration); (b) total crater depth - h and coating thickness - h_c (schematic illustration); (c) internal diameter - a and external diameter – b.[9]

The internal and external diameters of the wear crater are commonly measured by optical microscopy, but other methods are available. For example, Computer Aided Design (CAD) software[2,5] has been used for this purpose. The total wear volume and the total crater depth may be determined as a function of b, using Equations 1[10] and 2,[11] respectively, where R is the radius of the ball. These equations are also valid for non-coated systems.

$$V \cong \frac{\pi b^4}{64R} \qquad \text{for } b << R \qquad (1)$$

$$h \cong \frac{b^2}{8R} \qquad \text{for } b << R \qquad (2)$$

Two abrasive wear modes are usually observed on the surface of the worn crater: “rolling abrasion” results when the abrasive particles roll on the specimen, while “grooving abrasion” is observed when the abrasive particles slide[12-15] on the specimen. Depending on test conditions, “rolling abrasion” and “grooving abrasion” can occur simultaneously in a given crater.[1,2,5,6,12-14] Figures 3a,[12] 3b and 3c[5] present, respectively, images of rolling abrasion, grooving abrasion and a simultaneous action of rolling and grooving abrasion.

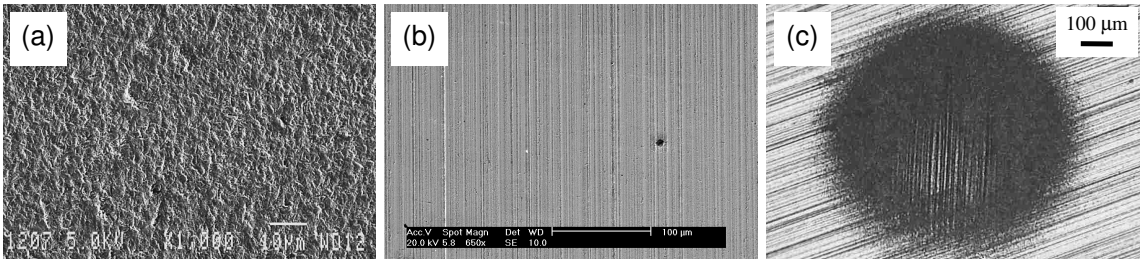

Figure 3. Abrasive wear modes: (a) rolling abrasion;[12] (b) grooving abrasion; (c) simultaneous action of rolling abrasion and grooving abrasion.[5]

The micro-abrasive wear test has been applied in the study of the abrasive wear of metallic[1-5,12] and non-metallic[5,6,15-23] materials and, depending on the equipment configuration, it is possible to apply normal loads (N) from 0.01 N[13,14] to 10 N[1,2,12,15,24-26] and ball rotational speeds (n) up to 80 rpm.[2,17-19]

The wear behavior of different materials is analyzed based on the dimensions of the wear crater and/or on the wear mode. Since the early works of Hutchings,[11-14,22,27] other important contributions have been provided in terms of this type of test, such as: the wear mode transition;[12-14] the wear coefficient (k);[17-19,21,26] micro-abrasive wear of coated systems;[17-19,21-23,26-32] micro-contact modelling of abrasive wear,[33-42] ridge formation[24;25,43-45] and angularity of abrasive particles.[46,47]

Many works on friction coefficient (μ) during abrasive wear and other types of tests are available in the literature,[48-62] but only a few were dedicated to the friction coefficient in micro-abrasive wear tests with rotating ball.[22,36,44,63,64] In particular, Shipway[36] has analyzed the friction coefficient in terms of the shape and movement of the abrasive particles, Kusano and Hutchings[63] presented a theroretical model for friction coefficient in micro-abrasive wear tests with free ball equipment configuration and Cozza, Tanaka e Souza[65] measured the tangential force developed during tests conducted in a fixed ball equipment configuration, which allowed direct calculation of the friction coefficient by the ratio between the tangential and normal forces.

With the intent to colaborate with the understanding of the behavior of the friction coefficient and wear coefficient of thin films in micro-scale abrasion wear tests by rotative ball, this work has two purposes: to study the influence of TiN and TiC coatings hardness on the i) friction coefficient and ii) wear coefficient.

2 EXPERIMENTAL DETAILS

2.1 Micro-abrasive Wear Test Equipment

An equipment with fixed-ball configuration (Figure 4) was used in the micro-scale abrasive wear tests. This equipment was designed and assembled with some mechanical and electrical differences from fixed-ball equipments found in the literature.[12-15,17-19,24-26,30,31,43-45,61,66-68]

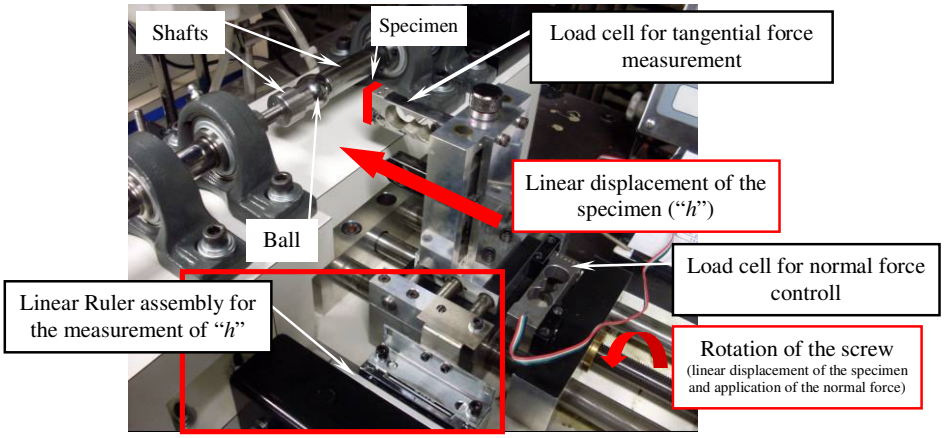

Figure 4. Micro-abrasive wear test equipment with fixed-ball configuration[65] used in the experiments of this work. Specimen: schematic illustration.

In the test apparatus used in this work, the ball is fixed by two shafts, similar to systems available commercially,[14,38,68] and their rotation (shafts and ball) is controlled by a couple "servo-motor / servo-controller", bought from Rexroth Bosch Group. This system allows to select rotational speeds of the ball from 10^{-5} rpm up to 9,000 rpm, in both directions (clockwise and counter-clockwise). It is important to mention that the ball presents an eccentricity (misalignment) between 21-27 μm, without load. This condition was also observed by Gee and Wicks[44] but with a slightly lower eccentricity, between 20-24 μm.
The normal force, controlled by a load cell, is applied on the specimen with the help of a second couple "servo-motor / servo-controller" (also provided by Rexroth Bosch Group); it rotates a screw and the normal force is applied. The tangential force (T) generated during the tests is measured by a second load cell, fixed below of the specimen, and its value is shown by a readout system.
Finally, with the help of a Linear Ruler, it is possible to continuously measure the displacement of the specimen (or, wear crater depth - h) during the tests, with precision of 1 μm.

2.2 Materials

Experiments were conducted with one ball made of AISI 52100 steel, which presented a diameter (D) of 25.4 mm (1"). Two specimens of AISI D2 tool steel, one coated with titanium nitride (TiN) and the other coated with titanium carbide (TiC), were used in the tests.
The thin films were depostied at the Instituto Tecnológico de Aeronáutica (ITA), in a Reactive Diode RF Magnetron Sputtering chamber. Table 1 shows the parameters that were kept constant during the depositions and Table 2 presents the individual

deposition conditions, the thickness (h_c) of the thin films and their reduced Young's modulus (E^*). The values of E^* were calculated based on nanoindentation data and these values allow the calculation of the elastic modulus of the thin film, through Equation 3.

Table 1. Constant parameters of deposition of the TiN and TiC coatings.

(a) Parameter	Condition (b)
Temperature	350 °C
Polarization voltage	0 V
RF generator power apllied about the magnetron catode	500 W
Initial pressure of Ar	3 mTorr
Base pressure	2.10^{-6} Torr

Table 2. Conditions of deposition of the TiN and TiC coatings.

Thin film	Flux of N_2 [sccm]	Flux of CH_4 [sccm]	$\frac{F_{N_2}}{F_{N_2}+F_{Ar}}$	$\frac{F_{CH_4}}{F_{CH_4}+F_{Ar}}$	Pressure [mTorr]	Time [min]	h_c [µm]	E^* [GPa]
TiN	6.0	–	0.23	–	3.5	165.0	2.0	270.9
TiC	–	5.0	–	0.19	2.5	105.0	2.3	135.1

$$\frac{1}{E^*} = \frac{1-\nu_c^2}{E_c} + \frac{1-\nu_i^2}{E_i} \qquad (3)$$

E_c, ν_c, E_i and ν_i are the Young's modulus and the coefficient of Poisson of the coating and indenter, respectively.

Table 3 presents the hardness (H) values of the materials used in this work (substrate, thin films, ball[2,5,6,65] and abrasive particles[2,5,6,69]). The values for the thin films were also calculated based on nanoindentation data.

Table 3. Hardness of the materials used in this work.

	Material	Hardness - H [GPa (HV)]
Substrate	AISI D2 tool steel	7.3 (744)
Thin film [1]	TiN	25.6
	TiC	14.3
Ball	AISI 52100 steel	8.4 (856)[2,5,6,65]
Abrasive particles	SiC	18.5 - 19 (1886 - 1937)[2,5,6,69]

(1) The thin film hardness was measured with a Berkovich indenter.

The abrasive used was black silicon carbide (SiC) with average particle size of 5 µm.[2,5,6,69] Figure 5[69] presents a micrograph of abrasive particles (Figure 5a) and particle size distribution (Figure 5b). The abrasive slurry was prepared as a mixture of 25% of SiC and 75% of distilled water, in volume. This mixture results in 1.045 g of SiC per cm^3 of distilled water.[1,2,5,6,65]

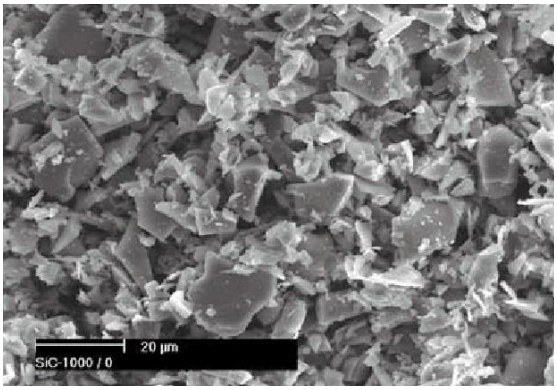

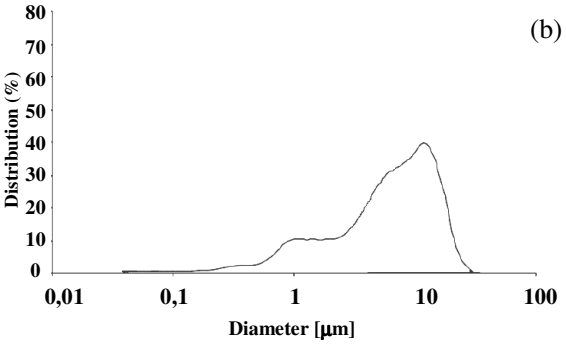

Figure 5. SiC abrasive:[69] (a) scanning electron micrograph; (b) particle size distribution.

2.3 Micro-abrasive Wear Tests

Table 4 shows the test conditions selected for the experiments conducted in this work.

Table 4. Test conditions selected for the wear experiments.

Test condition ⇒	1	2	3	4	5	6
Normal force - N_1 [N]	1.25	1.25	1.25	1.25	1.25	1.25
Normal force - N_2 [N]	5	5	5	5	5	5
Sliding distance - S [m]	10	16	25	40	63	100
Ball rotational speed - n [rpm]	37.6	37.6	37.6	37.6	37.6	37.6
Tangential sliding velocity - v [m/s]	0.05	0.05	0.05	0.05	0.05	0.05
Test time - t	200 s (3 min 20 s)	320 s (5 min 20 s)	500 s (8 min 20 s)	800 s (13 min 20 s)	1,260 s (21 min)	2,000 s (33 min 20 s)
Number of repetitions	3	3	3	3	3	3

Two values of normal force were defined for the wear experiments: N_1 = 1.25 N and N_2 = 5 N.

The ball rotational speed was n = 37.6 rpm, which was previously selected by Trezona, Allsopp and Hutchings[12] and Adachi and Hutchings.[13,14] For n = 37.6 rpm and D = 25.4 mm (R = 12.7 mm), the tangential sliding velocity at the external diameter of the ball is equal to v = 0.05 m/s, which probably reduces or eliminates the occurrence of hidrodynamic effects during the tests.[14]

Tests were run for six different sliding distances (S), S_1 = 10 m, S_2 = 16 m, S_3 = 25 m, S_4 = 40 m, S_5 = 63 m and S_6 = 100 m. These values were based on the Renard's Series - R20/4[70]. The correspondent test times were, respectively, t_1 = 200 s (3 min 20 s), t_2 = 320 s (5 min 20 s), t_3 = 500 s (8 min 20 s), t_4 = 800 s (13 min 20 s), t_5 = 1,260 s (21 min) and t_6 = 2,000 s (33 min 20 s), as presented in Table 4.

The Linear Ruler presented in Figure 4 allowed constant monitoring of the crater depth (h), and thus the calculation of the wear volume, without the need to stop the test for crater dimension measuring. Three repetitions were conducted for each value of N, totalizing 12 experiments.

The abrasive slurry was continuously agitated and was manually fed to the specimen-ball contact, with the help of a dropper, at a rate of one drop every 20 s. This frequence is equal to that selected by Kusano and Hutchings.[63]

2.4 Data Acquisition and Result Analysis

The calculation of individual values for the wear volumes of the coating and the substrate was conducted based on the following procedure.
First, for each test time presented in Table 4, the respective crater depth (h) was measured (with the Linear Ruler), and from Equation 4,[12] the total wear volume (V) (coating and substrate) could be calculated:

$$V \cong \pi R h^2 \qquad \text{for } h << R \qquad (4)$$

The wear volume of the substrate (V_s) and the wear volume of the coating (V_c) were calculated from Equations 5 and 6, respectively.

$$V_s \cong \pi R (h - h_c)^2 \qquad \text{for } h << R \qquad (5)$$

$$V_c \cong \pi R (2 h h_c - h_c^2) \qquad \text{for } h << R \qquad (6)$$

The total wear coefficient (kt), the wear coefficient of the substrate (ks) and the wear coefficient of the coating (kc) were calculated from Equations 7, 8 and 9, respectively.

$$kt = \frac{\pi R h^2}{NS} \qquad (7)$$

$$ks = \frac{\pi R (h - h_c)^2}{NS} \qquad (8)$$

$$kc = \frac{\pi R (2 h h_c - h_c^2)}{NS} \qquad (9)$$

Values of normal load (N) and tangencial force (T) were registered during all the tests, once every t = 40 s. Then, the friction coefficient[1] was determined using Equation 10.

$$\mu = \frac{T}{N} \qquad (10)$$

For each specimen ("AISI D2 tool steel coated with TiN" and "AISI D2 tool steel coated with TiC"), the three curves of friction coefficient as a function of the test time ($\mu = f(t)$) obtained under N_1 = 1.25 N were compared with the three curves of $\mu = f(t)$ obtained under N_2 = 5 N through ANOVA (Analysis of Variance[71-73]), with a significance level (α) of 10%.
Later, the six $\mu = f(t)$ curves produced on the "AISI D2 tool steel + TiN" were compared with the six $\mu = f(t)$ curves produced on the "AISI D2 tool steel + TiC", also through ANOVA and α = 10%.

[1] The term "friction coefficient" was adopted in this work, since it is the most usual designation of the ratio between tangential and normal forces.

3 RESULTS AND DISCUSSION

3.1 Abrasive Wear Modes

Optical microscopy analysis of the wear craters obtained in this work indicated that, in all cases, the abrasive wear mode was grooving abrasion. Figures 6a and 6b present SEM images of the centre of the wear craters produced on the AISI D2 tool steel specimen coated with TiN, under N_1 = 1.25 N and N_2 = 5 N, respectively. Figures 6c and 6d present images of the centre of the wear craters generated on the substrate coated with TiC, for N_1 = 1.25 N and N_2 = 5 N, respectively. In all the cases, the tests were perforating, *i.e.* the final crater depth was larger than the film thickness.

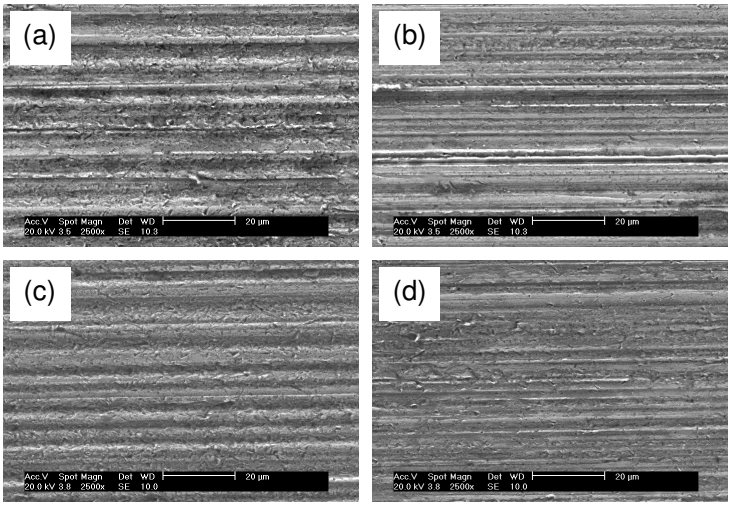

Figure 6. Occurrence of grooving abrasion. (a) and (b): AISI D2 tool steel coated with TiN, normal force of 1.25 N and 5 N, respectively; (c) and (d): AISI D2 tool steel coated with TiC, normal force of 1.25 N and 5 N, respectively. Sliding distance of 100 m.

3.2 Friction Coefficient Behavior

Figure 7 presents the behavior of the friction coefficient (μ) as a function of the test time, for both AISI D2 tool steel specimens coated with TiN and TiC. In this figure, trend lines were drawn to approximately indicate the borders of the region with the experimental friction coefficient values. Two quantities, μ_{higher} and μ_{lower}, were defined as the value of the upper and lower trend lines, respectively, for t_6 = 2,000 s; this procedure was equally conducted by Cozza, Tanaka e Souza.[65]

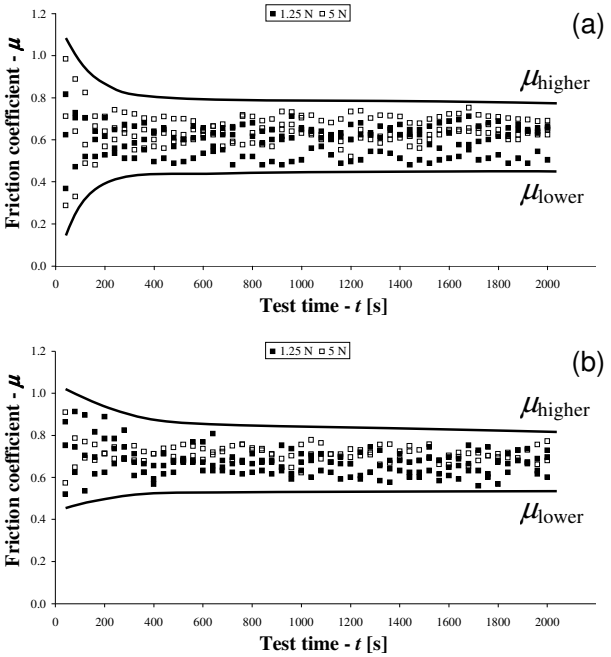

Figure 7. Friction coefficient as a function of the test time. AISI D2 tool steel coated with (a) TiN and (b) TiC.

For both "AISI D2 tool steel + TiN" and "AISI D2 tool steel + TiC" and for both both N_1 = 1.25 N and N_2 = 5 N, the friction coefficient range remained from μ = 0.4 to μ = 0.9. With the AISI D2 tool steel coated with TiN, it was observed a ratio between the higher friction coefficient and the lower friction coefficient of $\mu_{higher}/\mu_{lower} \cong 1.8$, and with the AISI D2 coated with TiC, the value was $\mu_{higher}/\mu_{lower} \cong 2$.
Through ANOVA, it was observed that:

(i) "AISI D2 + TiN": for both N_1 = 1.25 N and N_2 = 5 N, the friction coefficient values obtained are statistically different. Figure 7a indicates that the friction coefficient values were slightly larger for N_2 = 5 N.
(ii) "AISI D2 + TiC": for both N_1 = 1.25 N and N_2 = 5 N, the friction coefficient values obtained are statistically different. Figure 7b indicates that the friction coefficient values were slightly larger for N_2 = 5 N.
(iii) Comparison between "AISI D2 + TiN" and "AISI D2 + TiC": for both N_1 = 1.25 N and N_2 = 5 N, the friction coefficient values obtained are statistically different.

3.3 Relationship Between Hardness and Friction Coefficient

The hardness of a material affects the occurrence of rolling abrasion and/or grooving abrasion, as described in the wear map of Adachi and Hutchings.[13;14] Besides, the abrasive wear mode might have an important role on the friction coefficient values. Kusano and Hutchings[63], conducting ball-cratering abrasive wear tests in a test apparatus with "free-ball" configuration, obtained values of friction coefficient of approximately μ = 0.2, under conditions of *rolling abrasion*. On the other hand, Cozza, Tanaka e Souza[65] observed higher values, from μ = 0.2 to μ = 1.2, in a test device with "fixed-ball" configuration and under conditions of *grooving abrasion*.
The range of friction coefficient values obtained in this work (from μ = 0.4 to μ = 0.9) is included in the range obtained in the previous work of Cozza, Tanaka e Souza[65]

(from μ = 0.2 to μ = 1.2) and it may be related with the occurrence of grooving abrasion.
In terms of the specimens analyzed in this work, the substrate (AISI D2 tool steel) was the same for both TiN and TiC coated specimens and then it is probably correct to say that its hardness had the same influence on the occurrence of the abrasive wear mode (grooving abrasion in all experiments) and on the friction coefficient behavior. In fact, although the curves $\mu = f(t)$ are statistically different, the average values are similar ("AISI D2 tool steel + TiN": 0.6 and 0.65, to 1.25 N and 5 N, respectively; "AISI D2 tool steel + TiC": 0.67 and 0.74, to 1.25 N and 5 N, respectively). Thus, in this work, the hardness of the coatings did not have a significant influence on the friction coefficient values as a function of the test time.

3.4 Wear Coefficient Behavior

Figure 8 presents the behavior of the wear coefficient as a function of the test time, for the "AISI D2 tool steel coated with TiN" and "AISI D2 tool steel coated with TiC". This figure shows the total wear coefficient (kt) (substrate + coating), the wear coefficient of the substrate (ks) and the wear coefficient of the coating (kc).

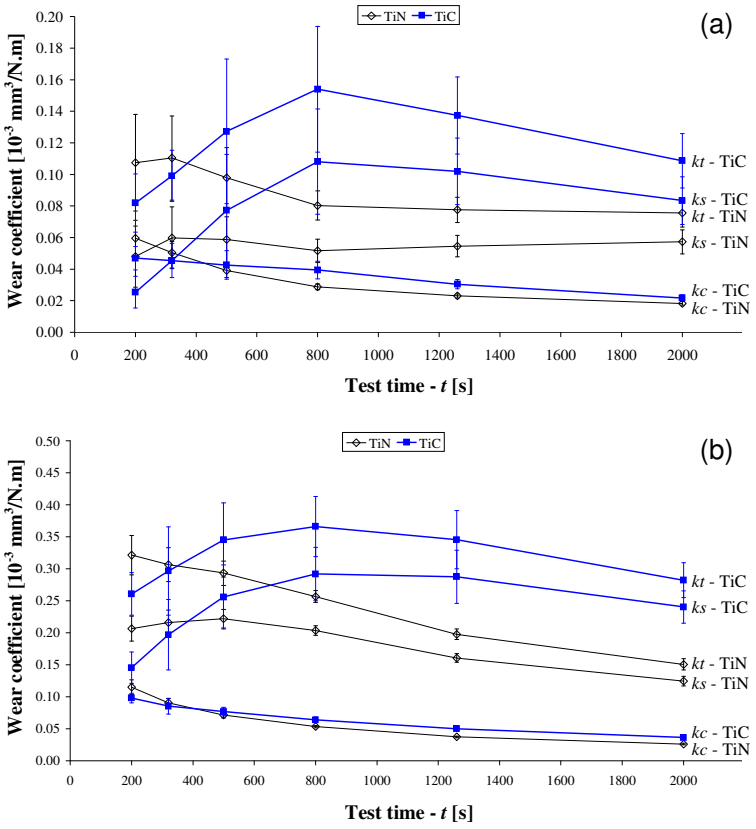

Figure 8. Wear coefficient as a function of the test time. (a) N_1 = 1.25 N - TiN and TiC coatings; (b) N_2 = 5 N - TiN and TiC coatings.

For both "AISI D2 tool steel + TiN" and "AISI D2 tool steel + TiC", the application of the normal force N_2 = 5 N resulted in higher values of kt, ks and kc than with N_1 = 1.25 N, what is a result with qualitative agreement with the literature[15;74]; higher

normal forces favor higher wear coefficients and lower normal forces favor lower wear coefficients.

Analyzing Figures 8a and 8b, it is possible to note that, for both TiN and TiC coatings, the wear coefficients of the coatings (kc - TiC and kc - TiN) are similar for the two values of normal force. This similarity is related to a similarity in film thickness (2.0 μm and 2.3 μm, TiN and TiC, respectively), which provides similar wear volumes. Nevertheless, it is important to notice that, from approximately 400 s, the wear coefficient kc of the coating with the lowest hardness (TiC) was consistently higher than that with the highest hardness (TiN).

Each specimen presented a distinct behavior in terms of the wear coefficient (kt and ks) as a function of the test time. For the "AISI D2 tool steel + TiN", the total wear coefficient and the wear coefficient of the substrate decreased as a function of the test time, while the kt and ks values for the "AISI D2 tool steel + TiC" presented a maximum point at about t_4 = 800 s. In micro-abrasive wear tests it is usually recommended to conduct a comparison between two tested materials only after the steady state of wear is achieved, *i.e.* after the point where no significant variation in wear coefficient is observed as a function of time. This idea opposes a direct comparison between the values of ks and kt in Figure 8, since the steady state of wear was not achieved in some cases, especially with the TiC-coated specimen. On the other hand, some work must be dedicated to the understanding of why two coated specimens with the same substrate material presented such difference in behavior.

4 CONCLUSIONS

The results obtained in this work have indicated that:

(1) The hardness of the coatings did not have a significant influence on the friction coefficient values; they remained in the same range, from μ = 0.4 to μ = 0.9, and with average values between 0.6 and 0.74. Besides, for both "AISI D2 tool steel + TiN" and "AISI D2 tool steel + TiC" the friction coefficient curves presented, practically, the same behavior, independent of the hardness of the coatings.

(2) The TiN-coated specimen (higher hardness) presented lower wear coefficient values (kt, ks and kc) than the TiC-coated specimen. In terms of the wear coefficient of the coating kc, the difference may be associated either with the higher thickness or to the lower hardness of the TiC coating. No conclusion can be drawn with respect to the ks values, since the steady state of wear was not achieved in some cases, especially with the TiC-coated specimen.

Acknowledgements

The authors gratefully acknowledge Prof. Maria Helena Santos Takeda, from Polytechnic School of the University of São Paulo, for the help in the statistics analysis; Prof. José Carlos Bressiani, from Nuclear and Energetic Researches Institute, for the silicon carbide and the abrasive particle size distribution analysis; Paulo Zanini, Rafael Rozolen and Vitor Benkard Lira, from Rexroth Bosch Group, for the help in the start-up of the servo-motors and servo-controllers.

REFERENCES

1 COZZA, R.C.; SOUZA, R.M.; TANAKA, D.K. Wear mode transition during the micro-scale abrasion of WC-Co P20 and M2 tool steel. IN: PROCEEDINGS OF THE XVIII INTERNATIONAL CONGRESS OF MECHANICAL ENGINEERING, Ouro Preto - MG, Brazil, 2005.

2 COZZA, R.C. Wear coefficient and wear mode transition study in micro-abrasive wear testing, M.Sc. Dissertation, Polytechnic School of the University of São Paulo, São Paulo - SP, Brazil, 2006, 217 p. (in Portuguese).

3 DA SILVA, W.M. Effect of pressing pressure and iron powder size on the micro-abrasion of steam-oxidized sintered iron, M.Sc. Dissertation, Federal University of Uberlândia, Uberlândia - MG, Brazil, 2003, 98 p.(in Portuguese).

4 DA SILVA, W.M.; BINDER, R.; DE MELLO, J.D.B. Abrasive wear of steam-treated sintered iron, Wear 258 (2005) 166-177.

5 COZZA, R.C.; DE MELLO, J.D.B.; TANAKA, D.K.; SOUZA, R.M. Relationship between test severity and wear mode transition in micro-abrasive wear tests, Wear 263 (2007) 111-116.

6 COZZA, R.C.; TANAKA, D.K.; SOUZA, R.M. Micro-abrasive wear of DC and pulsed DC titanium nitride thin films with different levels of film residual stresses, Surface and Coatings Technology 201 (2006) 4242-4246.

7 COZZA, R.C.; SOUZA, R.M.; TANAKA, D.K. Ball wear influence at the caps formation in the micro-abrasive wear testing by rotative fix ball. IN: PROCEEDINGS OF THE IV NATIONAL CONGRESS OF MECHANICAL ENGINEERING, Recife - PE, Brazil, 2006 (in Portuguese).

8 ZEFERINO, R.R.F.; COZZA, R.C.; SOUZA, R.M.; TANAKA, D.K. Effect of the contact pressure on the wear mode transition in micro-abrasive wear tests of WC-Co P20. IN: PROCEEDINGS OF THE IXX INTERNATIONAL CONGRESS OF MECHANICAL ENGINEERING, Brasília - DF, Brazil, 2007.

9 COZZA, R.C.; DE SOUZA, L.F.M.; ZEFERINO, R.R.F.; DAS NEVES, M.D.M.; SOUZA, R.M.; TANAKA, D.K. A study about results reprodutibility and abrasive particles fragmentation in micro-abrasive wear testing by rotating ball. IN: PROCEEDINGS OF THE V NATIONAL CONGRESS OF MECHANICAL ENGINEERING, Salvador - BA, Brazil, 2008 (in Portuguese).

10 KELLY, D.A.; HUTCHINGS, I.M. A new method for measurement of particle abrasivity, Wear 250 (2001) 76-80.

11 RUTHERFORD, K.L.; HUTCHINGS, I.M. Theory and application of a micro-scale abrasive wear test, Journal of Testing and Evaluation - JTEVA 25 (2) (1997) 250-260.

12 TREZONA, R.I.; ALLSOPP, D.N.; HUTCHINGS, I.M. Transitions between two-body and three-body abrasive wear: influence of test conditions in the microscale abrasive wear test, Wear 225-229 (1999) 205-214.

13 ADACHI, K.; HUTCHINGS, I.M. Wear-mode mapping for the micro-scale abrasion test, Wear 255 (2003) 23-29.

14 ADACHI, K.; HUTCHINGS, I.M. Sensitivity of wear rates in the micro-scale abrasion test to test conditions and material hardness, Wear 258 (2005) 318-321.

15 BOSE, K.; WOOD, R.J.K. Optimun tests conditions for attaining uniform rolling abrasion in ball cratering tests on hard coatings, Wear 258 (2005) 322-332.

16 MERGLER, Y.J.; HUIS IN 'T VELD, H. Micro-abrasive wear of semi-crystalline polymers, Tribological Research and Design for Engineering Systems (2003) 165-173.

17 BATISTA, J.C.A.; MATTHEWS, A.; GODOY, C. Micro-abrasive wear of PVD duplex and single-layered coatings, Surface and Coatings Technology 142-144 (2001) 1137-1143.

18 BATISTA, J.C.A.; GODOY, C.; MATTHEWS, A. Micro-scale abrasive wear testing of duplex and non-duplex (single-layered) PVD (Ti,Al)N, TiN and Cr-N coatings, Tribology International 35 (2002) 363-372.
19 BATISTA, J.C.A.; JOSEPH, M.C.; GODOY, C.; MATTHEWS, A. Micro-abrasion wear testing of PVD TiN coatings on untreated and plasma nitrided AISI H13 steel, Wear 249 (2002) 971-979.
20 BAPTISTA, A.M.; FERREIRA, J.; PINTO, N. Micro-abrasive wear testing by rotating ball, 7th Portuguese Conference of Tribology, Porto, Portugal, 2000 (in Portuguese).
21 BELLO, J.O.; WOOD, R.J.K. Micro-abrasion of filled and unfilled polyamide 11 coatings, Wear 258 (2005) 294-302.
22 RUTHERFORD, K.L.; HUTCHINGS, I.M. A micro-abrasive wear test, with particular application to coated systems, Surface and Coatings Technology 79 (1996) 231-239.
23 RAMALHO, A. Micro-scale abrasive wear of coated surfaces-prediction models, Surface and Coatings Technology 197 (2005) 358-366.
24 SHIPWAY, P.H.; HODGE, C.J.B. Microabrasion of glass - the critical role of ridge formation, Wear 237 (2000) 90-97.
25 GEE, M.G.; GANT, A.; HUTCHINGS, I.M.; BETHKE, R.; SCHIFFMAN, K.; VAN ACKER, K.; POULAT, S.; GACHON, Y.; VON STEBUT, J. Progress towards standardisation of ball cratering, Wear 255 (2003) 1-13.
26 BELLO, J.O.; WOOD, R.J.K. Grooving micro-abrasion of polyamide 11 coated carbon steel tubulars for downhole application, Wear 255 (2003) 1157-1167.
27 HUTCHINGS, I.M. Abrasive and erosive wear tests for thin coatings: a unified approach, Tribology International 31 (1-3) (1998) 5-15.
28 KUSANO, Y.; VAN ACKER, K.; HUTCHINGS, I.M. Methods of data analysis for the micro-scale abrasion test on coated substrates, Surface and Coatings Technology 183 (2004) 312-327.
29 ALLSOPP, D.N.; HUTCHINGS, I.M. Micro-scale abrasion and scratch response of PVD coatings at elevated temperatures, Wear 251 (2001) 1308-1314.
30 SHIPWAY, P.H.; HOWELL, L. Microscale abrasion-corrosion behaviour of WC-Co hardmetals and HVOF sprayed coatings, Wear 258 (2005) 303-312.
31 CHEN, H.; XU, C.; ZHOU, Q.; HUTCHINGS, I.M.; SHIPWAY, P.H.; LIU, J. Micro-scale abrasive wear behaviour of HVOF sprayed and laser-remelted conventional and nanostructured WC-Co coatings, Wear 258 (2005) 333-338.
32 RUTHERFORD, K.L.; HUTCHINGS, I.M. Micro-scale abrasive wear testing of PVD coatings on curved substrates, Tribology Letters 2 (1996) 1-11.
33 WILLIAMS, J.A. Wear modelling: analytical, computational and mapping: a continuum mechanics approach, Wear 225-229 (1999) 1-17.
34 HISAKADO, T.; TANAKA, T.; SUDA, H. Effect of abrasive particle size on fraction of debris removed from plowing volume in abrasive wear, Wear 236 (1999) 24-33.
35 FANG, L.; XING, J.; LIU, W.; XUE, Q.; WU, G.; ZHANG, X. Computer simulation of two-body abrasion process, Wear 251 (2001) 1356-1360.
36 SHIPWAY, P.H. A mechanical model for particle motion in the micro-scale abrasion wear test, Wear 257 (2004) 984-991.
37 MASEN, M.A.; DE ROOIJ, M.B.; SCHIPPER, D.J. Micro-contact based modelling of abrasive wear, Wear 258 (2005) 339-348.
38 SINNETT-JONES, P.E.; WHARTON, J.A.; WOOD, R.J.K. Micro-abrasion-corrosion of a CoCrMo alloy in simulated artificial hip joint environments, Wear 259 (2005) 898-904.
39 GORANA, V.K.; JAIN, V.K.; LAL, G.K. Forces prediction during material deformation in abrasive flow machining, Wear 260 (2006) 128-139.
40 BARGE, M.; RECH, J.; HAMDI, H.; BERGHEAU, J.M. Experimental study of abrasive process, Wear 264 (2008) 382-388.
41 WILLIAMS, J.A.; HYNCICA, A.M. Abrasive wear in lubricated contacts, Journal of Physics D: Applied Physics 25 (1992) A81-A90.
42 KATO, K. Abrasive wear of metals, Tribology International 30 (5) (1997) 333-338.

43 TREZONA, R.I.; HUTCHINGS, I.M. Three-body abrasive wear testing of soft materials, Wear 233-235 (1999) 209-221.
44 GEE, M.G.; WICKS, M.J. Ball crater testing for the measurement of the unlubricated sliding wear of wear-resistant coatings, Surface and Coatings Technology 133-134 (2000) 376-382.
45 ALLSOPP, D.N.; TREZONA, R.I.; HUTCHINGS, I.M. The effects of ball surface condition in the micro-scale abrasive wear test, Tribology Letters 5 (1998) 259-264.
46 STACHOWIAK, G.W. Particle angularity and its relationship to abrasive and erosive wear, Wear 241 (2000) 214-219.
47 STACHOWIAK, G.B.; STACHOWIAK, G.W. Wear mechanisms in ball-cratering tests with large abrasive particles, Wear 256 (2004) 600-607.
48 MERCER, A.P.; HUTCHINGS, I.M. The influence of atmospheric humidity on the abrasive wear of metals, Wear 103 (1985) 205-215.
49 MERCER, A.P.; HUTCHINGS, I.M. The influence of atmospheric composition on the abrasive wear of titanium and Ti-6Al-4V, Wear 124 (1988) 165-176.
50 MERCER, A.P.; HUTCHINGS, I.M. The deterioration of bonded abrasive papers during the wear of metals, Wear 132 (1989) 77-97.
51 KATO, K. Micro-mechanisms of wear - wear modes, Wear 153 (1992) 277-295.
52 XIE, Y.; WILLIAMS, J.A. The prediction of friction and wear when a soft surface slides against a harder rough surface, Wear 196 (1996) 21-34.
53 KATO, K. Wear in relation to friction - a review, Wear 241 (2000) 151-157.
54 NEVILLE, A.; KOLLIA-RAFAILIDI, V. A comparison of boundary wear film formation on steel and a thermal sprayed Co/Cr/Mo coating under sliding conditions, Wear 252 (2002) 227-239.
55 WANG, L.; WOOD, R.J.K.; HARVEY, T.J.; MORRIS, S.; POWRIE, H.E.G.; CARE, I. Wear performance of oil lubricated silicon nitride sliding against various bearing steels, Wear 255 (2003) 657-668.
56 DHANASEKARAN, S.; GNANAMOORTHY, R. Abrasive wear behavior of sintered steels prepared with MoS_2 addition, Wear 262 (2007) 617-623.
57 YAN, Y.; NEVILLE, A.; DOWSON, D. Tribo-corrosion properties of cobalt-based medical implant alloys in simulated biological environments, Wear 263 (2007) 1105-1111.
58 JIANXIN, D.; JIANHUA, L.; JINLONG, Z.; WENLONG, S.; MING, N. Friction and wear behaviors of the PVD ZrN coated carbide in sliding wear tests and in machining processes, Wear 264 (2008) 298-307.
59 LIU, C.S.; ZHENG, Z.Y.; WU, D.W.; YE, M.S.; GAO, P.; PENG, Y.G.; FAN, X.J. Sliding friction and wear properties of CN_X/TiN composite films, Tribology International 37 (2004) 721-725.
60 ILIU, I. Wear and micropitting of steel ball sliding against TiN coated steel plate in dry and lubricated conditions, Tribology International 39 (2006) 607-615.
61 CESCHINI, L.; PALOMBARINI, G.; SAMBOGNA, G.; FIRRAO, D.; SCAVINO, G.; UBERTALLI, G. Friction and wear behaviour of sintered steels submitted to sliding and abrasion tests, Tribology International 39 (2006) 748-755.
62 DA SILVA, C.H. Degradation of UHMWPE and POM due to the tribologic action against stainless steel and alumina, Ph.D. Thesis, Polytechnic School of the University of São Paulo, São Paulo - SP, Brazil, 2003, 294 p. (in Portuguese).
63 KUSANO, Y.; HUTCHINGS, I.M. Sources of variability in the free-ball micro-scale abrasion test, Wear 258 (2005) 313-317.
64 GEE, M.G. National Physical Laboratory, UK, private communication, 2003.
65 COZZA, R.C.; TANAKA, D.K.; SOUZA, R.M. Friction coefficient and abrasive wear modes in ball-cratering tests conducted at constant normal force and constant pressure – preliminary results, Accept for publication in Wear.
66 GEE, M.G.; GANT, A.J.; HUTCHINGS, I.M.; KUSANO, Y.; SCHIFFMAN, K.; VAN ACKER, K.; POULAT, S.; GACHON, Y.; VON STEBUT, J.; HATTO, P.; PLINT, G.

Results from an interlaboratory exercise to validate the micro-scale abrasion test, Wear 259 (2005) 27-35.
67 SHIPWAY, P.H.; HOGG, J.J. Dependence of microscale abrasion mechanisms of WC-Co hardmetals on abrasive type, Wear 259 (2005) 44-51.
68 MATHEW, M.T.; STACK, M.M.; MATIJEVIC, B.; ROCHA, L.A.; ARIZA, E. Micro-abrasion resistance of thermochemically treated steels in aqueous solutions: Mechanisms, maps, materials selection, Tribology International 41 (2008) 141-149.
69 IZHEVSKYI, V.A.; GENOVA, L.A.; BRESSIANI, J.C.; BRESSIANI, A.H.A. Liquid phase sintered SiC ceramics from starting materials of different grade, Cerâmica 50 (2004) 261-267.
70 Standard DIN 804 - Edition: March/1977.
71 BOX, G.E.P.; HUNTER, J.S.; HUNTER, W.G. Statistics for Experimenters - Design, Innovation, and Discovery, 2nd Edition, John Wiley & Sons, Inc., Hoboken - New Jersey, USA, 2005.
72 VIEIRA, S. Analysis of Variance - ANOVA, 1st Edition, Editora Atlas S.A., São Paulo - SP, Brazil, 2006 (in Portuguese).
73 GUIMARÃES, P.S. Adjust of experimental curves, 1st Edition, Editora UFSM, Santa Maria - RS, Brazil, 2001 (in Portuguese).
74 BOSE, K.; WOOD, R.J.K. Influence of load and speed on rolling micro-abrasion of CVD diamond and other hard coatings, Diamond and Related Materials 12 (2003) 753-756.